J. Biochem. 2016;159(6):619–629 doi:10.1093/jb/mvw003

JB THE JOURNAL OF BIOCHEMISTRY

Physicochemical and biological characterizations of Pxt peptides from amphibian (*Xenopus tropicalis*) skin

Received November 3, 2015; accepted December 15, 2015; published online January 22, 2016

Yasushi Shigeri[1,*], Masanori Horie[1], Tsuyoshi Yoshida[1], Yoshihisa Hagihara[1], Tomohiro Imura[2], Hidetoshi Inagaki[3], Yoshikazu Haramoto[4], Yuzuru Ito[4] and Makoto Asashima[4]

[1]Health Research Institute, National Institute of Advanced Industrial Science and Technology, 1-8-31 Midorigaoka, Ikeda, Osaka 563-8577, Japan; [2]Research Institute for Chemical Process Technology, National Institute of Advanced Industrial Science and Technology, Tsukuba Central 5-2, 1-1-1 Higashi, Tsukuba, Ibaraki 305-8565, Japan; [3]Biomedical Research Institute, National Institute of Advanced Industrial Science and Technology, Tsukuba Central 6, 1-1-1 Higashi, Tsukuba, Ibaraki 305-8566 Japan; and [4]Biotechnology Research Institute for Drug Discovery, National Institute of Advanced Industrial Science and Technology, Tsukuba Central 4, 1-1-1 Higashi, Tsukuba, Ibaraki 305-8562, Japan

*Yasushi Shigeri, Health Research Institute, National Institute of Advanced Industrial Science and Technology, 1-8-31 Midorigaoka, Ikeda, Osaka 563-8577, Japan. Tel: +81-72-751-8324, Fax: +81-72-751-9517, email: yasushi.shigeri@aist.go.jp

Pxt peptides (Pxt-1 through Pxt-12) have been isolated from amphibian, *Xenopus tropicalis*. Pxt-related peptides (Pxt-2, Pxt-5, Pxt-12, reverse Pxt-2, reverse Pxt-5 and reverse Pxt-12) with significant foaming properties were further characterized. In the physicochemical experiments, all Pxt-related peptides formed significant amphiphilic α-helices in 50% 2,2,2-trifluoroethanol by circular dichroism measurements. Among Pxt-related peptides, both Pxt-5 and reverse Pxt-5 were the most effective in reducing their surface tensions. Moreover, Pxt-2, Pxt-5 and reverse Pxt-5 produced constant surface tensions above their critical association concentrations, suggesting the micelle-like assemblies. In the biological experiments, Pxt-5 possessed the most potent hemolytic activity, while reverse Pxt-5 exhibited the most remarkable gene expression of interleukin 8 and heme oxygenase 1 and the most potent cytotoxicity in HaCaT cells. In contrast, Pxt-12 and reverse Pxt-12 were much weaker in antimicrobial assays for Gram-negative bacteria, Gram-positive bacteria and yeasts, as well as in hemolytic, cell viability and cytotoxicity assays in HaCaT cells. All Pxt-related peptides exhibited about 20–50% of the total cellular histamine release at 10^{-5} M, as well as mastoparan and melittin in mast cells. Real-time polymerase chain reaction analysis confirmed the gene expressions of Pxt-5 in testis and Pxt-12 in muscle, in addition to skin, while Pxt-2 was only in skin.

Keywords: amphiphilic α-helical peptides/antimicrobial peptide/expression/surface tension/*Xenopus tropicalis*.

Abbreviations: AMPs, antimicrobial peptides; CD, circular dichroism; GRAVY, grand average of hydropathy; HMOX-1, heme oxygenase 1; IL-8, interleukin 8; LDH, lactate dehydrogenase; MALDI-MS, matrix-assisted laser desorption/ionization mass spectrometry; MIC, minimum inhibitory concentration; MTT, 3-(4,5-dimethyl-2-thiazolyl)-2,5-diphenyltetrazolium bromide; TFE, 2,2,2-trifluoroethanol.

Skin secretions from many kinds of amphibians have been actively investigated to isolate functional substances, such as antimicrobial peptides (AMPs) (*1*). For example, brevinin peptides, dermaseptin and magainin peptides were isolated from *Rana brevipoda* (*2*), *Phyllomedusa sauvagii* (*3*) and *Xenopus laevis* (*4*), respectively. At least 989 AMPs from amphibians have been discovered and registered in the Antimicrobial Peptide Database (http://aps.unmc.edu/AP/main.php) (*5*, *6*). Although their biological activities, such as antimicrobial and hemolytic effects on other organisms, are somewhat known, their primary physiological roles *in vivo* still remain a mystery.

Xenopus tropicalis, a species of frog in the Pipidae family, has been used frequently as a model organism for genetic and developmental research. Due to its shorter generation time and diploid genome, it was among the first amphibian genomes to be sequenced in 2010 (http://www.xenbase.org/entry/) (*7*). Before the release of its genome analysis data, Ali *et al.* (*8*) reported seven novel peptides (XT-1 through XT-7) with antimicrobial activity that were isolated from norepinephrine-stimulated skin secretions of *X.tropicalis*. However, with the exception of the fragment of XT-6 (identical to XT-6-like precursor), the amino acid sequences corresponding to XT peptides did not coincide with its genome analysis data. In 2013, after the release of its genome analysis data, Roelants *et al.* (*9*) conducted transcriptome, genome, peptidome and phylogenic analyses of the *X.tropicalis* skin complementary DNA (cDNA) library and reported 13 transcriptionally active genes and 19 peptides. Among them, 13 peptides showed antimicrobial, hemolytic and growth-inhibitory activities for bacteria, yeast, *Trypanosoma*, erythrocyte and T-lymphocytes. In 2015, we combined matrix-assisted laser desorption/ionization mass spectrometry (MALDI-MS) using slices of skin tissues (direct tissue MALDI-MS analysis) and database searches of DNA and protein, and successfully isolated 12 peptides (Pxt-1 through Pxt-12) from the skin of *X.tropicalis*. Moreover, we confirmed their presence in *X.tropicalis* secretory skin fluids by conventional MALDI-MS and their gene

expression in *X.tropicalis* skin by real-time polymerase chain reaction (RT-PCR) (*10*). Six Pxt-peptides (Pxt-2, Pxt-3, Pxt-5, Pxt-7, Pxt-11 and Pxt-12) were completely identical to those (PFQa-St2, Magainin-St1, PFQa-St1, Levitide-St2, Levitide-St1 and CPF-St7, respectively) reported by Roelants *et al.* (*9*). But they detected three Pxt-peptides (Pxt-4, Pxt-9 and Pxt-10) as only fragment peptides and the rest of them (Pxt-1, Pxt-6 and Pxt-8) were not confirmed by their nanoLC-MS/MS analysis (*9*). Moreover, Pxt-1 and Pxt-8 were found as the C-terminal sequences of prepro-XPF-St1, while Pxt-6 was identified as the C-terminal sequence of prepro-XPF-St6 (*9*).

After the discovery of Pxt-peptides, we found remarkable foaming properties of Pxt-peptides, such as Pxt-2, Pxt-5 and Pxt-12, in the process of peptide synthesis and purification by high performance (pressure) liquid chromatography (HPLC). Moreover, we measured the decrease in surface tension of Pxt-peptides, like detergents, in a concentration-dependent manner (*10*). In this study, we focused on Pxt-related peptides (Pxt-2, Pxt-5, Pxt-12, reverse Pxt-2, reverse Pxt-5 and reverse Pxt-12) and further characterized their physicochemical and biological properties using histamine-releasing activities in rat peritoneal mast cells, as well as cytotoxic, inflammatory and oxidative stress effects on cultured HaCaT cells, a skin exposure model, in addition to further confirmation of gene expression, antimicrobial and hemolytic activities and circular dichroism (CD) measurements.

Materials and Methods

Materials

Fmoc amino acids were obtained from the Peptide Institute Inc. (Osaka, Japan). The 2,2,2-trifluoroethanol (TFE) and amphotericin B were from Nacalai Tesque Inc. (Kyoto, Japan). ISOGEN was purchased from NIPPON GENE (Tokyo, Japan).

Peptide synthesis

All peptides were synthesized by Fmoc peptide chemistry using a Shimadzu PSSM-8 automated peptide synthesizer (Shimadzu, Kyoto, Japan), and purified by reverse-phase HPLC on a C18 column (Wako Pure Chemical Industries, Ltd, Osaka, Japan). The identity and purity of the peptides were confirmed by MALDI-TOF MS using a Microflex AI mass spectrometer (Bruker Corporation, Yokohama, Japan), and CHCA as the matrix.

Circular dichroism measurements of Pxt-related peptides

CD measurements were made with a spectropolarimeter, model J-820 (JASCO Corporation, Tokyo, Japan), at a peptide concentration of 5×10^{-5} M in 10 mM Tris–HCl (pH 7.2) or 50% TFE. The CD measurements were collected four times and averaged using the same samples. All peptides were analysed at 10, 25 and 37°C. The α-helical contents of the peptides were calculated from $[\theta]_{222}$ values using the following equation proposed by Forood *et al.* (*11*).

$$f_{\mathrm{H}} = [\theta]_{222}/[-40,000\times(1-2.5/n)]\times 100$$

f_{H}, n and $[\theta]_{222}$ represent the α-helical content (%), the number of amino acid residues and the ellipticity (deg cm^2/dmol) at 222 nm, respectively.

Surface tension measurements of Pxt-related peptides

The surface tensions of Pxt-related peptides (Pxt-2, Pxt-5, Pxt-12, reverse Pxt-2, reverse Pxt-5 and reverse Pxt-12) and other peptides (magainin 1, mastoparan and melittin) were determined by the pendant drop method at 25°C using interfacial tensiometer (DM500; Kyowa Interface Science Co., Ltd, Saitama, Japan) and Drop Shape Analysis software of FAMAS version 2.01, as described previously (*12*).

Antimicrobial activity of Pxt-related peptides

The antimicrobial assay was carried out according to the method of Steinberg *et al.* (*13*, *14*). *Escherichia coli* NBRC14237 (Gram-negative bacterium), *Pseudomonas aeruginosa* NBRC12582 (Gram-negative bacterium), *Staphylococcus aureus* NBRC12732 (Gram-positive bacterium), *Micrococcus luteus* NBRC12708 (Gram-positive bacterium), *Saccharomyces cerevisiae* NBRC10217 (yeast) and *Candida albicans* NBRC1594 (yeast) were utilized to determine minimum inhibitory concentration (MIC) values of Pxt-related peptides and other peptides. The minimum concentration of the peptides that did not result in any detectable growth was defined as the MIC. All peptides were diluted with the solution containing 0.001% bovine serum albumin and 0.01% acetic acid.

Hemolytic activity of Pxt-related peptides

Heparinized rat whole blood from Wistar rats (male, 6 weeks old) was washed twice in PBS (100 mM NaCl, 7.5 mM Na_2HPO_4 and 2.5 mM NaH_2PO_4) by centrifugation at 900 g and suspended in PBS to a concentration of 0.5% (v/v). The hemolytic assay was carried out with Pxt-related peptides (10^{-7} to 10^{-4} M), as described previously (*14*). PBS and PBS containing 0.2% Triton X-100 were used as controls for 0% and 100% hemolysis, respectively.

Histamine-releasing activity of Pxt-related peptides

The histamine-releasing activity of Pxt-related peptides was determined with rat peritoneal mast cells with Pxt-related peptides (10^{-5} or 5×10^{-5} M), as described previously (*15*, *16*). The combined intra- and extracellular amount of histamine was defined as the total amount of histamine. Histamine-releasing activity was expressed as a ratio of the extracellular to the total amount of histamine. Spontaneous release of histamine in the absence of the peptides was 7.4 ± 1.5%.

Cell culture

Human keratinocyte HaCaT cells were purchased from the German Cancer Research Center (DKFZ, Heidelberg, Germany). The cells were cultured in Dulbecco's modified Eagle's medium (DMEM; Gibco, Thermo Fischer Scientific, MA, USA) supplemented with 10% heat-inactivated fetal bovine serum (GE Healthcare, Tokyo, Japan), 100 U/ml of penicillin, 100 μg/ml of streptomycin and 250 ng/ml of amphotericin B. DMEM cultures were placed in a 75 cm^2 flask (Corning, NY, USA) and incubated at 37°C in an atmosphere of 5% CO_2. For cellular examinations, cells were seeded in 96-well or 24-well plates (Corning) at 2×10^5 cells/ml and incubated for 24 h.

Measurement of the cell viability (3 -(4,5-dimethyl-2-thiazolyl)-2,5-diphenyltetrazolium bromide assay)

For the determination of mitochondrial activity, the 3 -(4,5-dimethyl-2-thiazolyl)-2,5-diphenyltetrazolium bromide (MTT) assay was used, as described previously (*17*). The HaCaT cells were seeded in a 96-well plate (Corning) at 2×10^5 cells/well. They were incubated for 24 h and then the culture medium was removed. Subsequently, Pxt-related peptides (10^{-5} to 10^{-3} M) were applied and the cells were incubated for a further 6 and 24 h. Then, cells were incubated with 0.5 mg/ml MTT (Nacalai Tesque) at 37°C for 2 h. Isopropyl alcohol containing 40 mM HCl was added to the culture medium (3:2 by volume). These components were mixed using a pipette until the formazan was completely dissolved. The optical density of formazan was measured at 570 nm using a microplate reader.

Measurements of lactate dehydrogenase release

HaCaT cells were exposed to Pxt-related peptides (10^{-5} to 10^{-3} M) for 24 h and then the culture supernatant was collected and applied to lactate dehydrogenase (LDH) assay, as described previously (*17*). In the LDH assays, LDH release was measured with a tetrazolium salt by using a Cytotoxicity Detection KitPLUS (LDH) (Roche Diagnostics GmbH, Mannheim, Germany) according to the manufacturer's protocol. The amount of formazan salt that formed was measured at 492 nm by using the microplate reader. The maximum amount of released LDH was determined by incubating the cells

with a lysis solution that was provided in the kit. The cytotoxicity was calculated as follows. Cytotoxicity (%) = (experimental value − low control)/(high control − low control) × 100. The low control, which refers to spontaneous LDH release, was determined as the LDH released from non-treated normal cells. The high control, which refers to the maximum LDH release, was determined as the LDH released from cells that were lysed by surfactant treatment.

Determination of interleukin 8 concentration

HaCaT cells were exposed to Pxt-related peptides (10^{-4}M) for 24 h and then the culture supernatant was collected and applied to interleukin 8 (IL-8) assay. IL-8 concentration was determined by ELISA using Human IL-8 ELISA Ready-SET-Go! (Affymetrix eBioscience Inc., CA, USA). The ELISA was performed according to the protocol provided by the manufacturer.

Measurement of gene expression of IL-8 and heme oxygenase 1

HaCaT cells were seeded in 6-well microplates and incubated for 24 h at 37°C. After the culture medium was removed, Pxt-related peptides (10^{-4}M) were applied, and the cells were incubated for 24 h. The expression of the target genes was determined by RT-PCR, as described previously (*17*, *18*). Total RNA was isolated from the cells using an RNeasy mini kit (Qiagen, Tokyo, Japan). The cDNA synthesis was carried out with a High Capacity cDNA Reverse Transcription kit (Thermo Fischer Scientific). RT-PCR was conducted by an Applied Biosystems 7300 RT-PCR system (Thermo Fischer Scientific), and PCR amplification was detected by a TaqMan® gene expression assay (Thermo Fischer Scientific). The messenger RNA (mRNA) levels of IL-8 and heme oxygenase 1 (HMOX-1) were analysed using the TaqMan gene expression assay (IDs: Hs00174103_m1 for IL-8 and Hs01110250_m1 for HMOX-1). The human β-actin gene (ID: Hs99999903_m1) was used as an endogenous control.

Analysing mRNA expression of Pxt peptides (Pxt-2, Pxt-5 and Pxt-12) in Xenopus tropicalis by RT-PCR

Total RNA was conventionally extracted from 13 tissues (testis, ovary, skin, brain, heart, kidney, muscle, spleen, lung, stomach, intestine, liver and pancreas) of *X.tropicalis* (5 years old, Nigerian line) using ISOGEN by homogenization (Physcotron; Microtec Co., Ltd., Chiba, Japan). cDNAs were synthesized from 1 μg of total RNA using the SuperScript® III reverse transcriptase (Life Technologies, Tokyo, Japan) and Oligo $(dT)_{15}$ primer (Roche Diagnostic, Tokyo, Japan). These cDNA products were used as templates. Pxt-2, Pxt-5, Pxt-12 and EF1 α were amplified using the following forward (Fw) and reverse (Rv) primers.

Fw for Pxt-2: 5′-CAACCTTGCCGCTTCTGTAAC-3′
Rv for Pxt-2: 5′-CCTACTGGCTGTGCCATTGA-3′
Fw for Pxt-5: 5′-AGACCCAGATGAGATGATTGAACG-3′
Rv for Pxt-5: 5′-AATGGACCAAGAAGTGCCCC-3′
Fw for Pxt-12: 5′-GGAAATGAATGAACGAGTAGCCC-3′
Rv for Pxt-12: 5′-GCCAAAATCCATCCAACCCTC-3′
Fw for EF1 α: 5′-TGTAGGAGTCATCAAGGCGGTC-3′
Rv for EF1 α: 5′-ACAGATTTTGGTCAAGTTGCTTCC-3′

An EF1 α gene was used as an internal standard for the RT-PCR analyses. PCR was performed for 35 cycles (denaturation for 30 s at 94°C, annealing for 30 s at 55°C and extension for 30 s at 72°C) of Pxt peptides (Pxt-2, Pxt-5 and Pxt-12) or 22 cycles (denaturation for 30 s at 94°C, annealing for 30 s at 60°C and extension for 30 s at 72°C) of EF1 α. The amplified fragments were subjected to 2% agarose gel electrophoresis in TAE buffer and stained with ethidium bromide.

Results

Physicochemical properties of Pxt-related peptides

Eleven of the 12 Pxt peptides (Pxt-1 through Pxt-11) from the skin of *X.tropicalis* (*10*) were characterized, but not the Pxt-12 peptide, since it was identical to the already-known *X.tropicalis* XT-6-like precursor (*8*, *9*, *19*). To further characterize the Pxt peptides, we performed the peptide synthesis of Pxt-12 and preliminarily found its significant foaming property. Then, we selected and synthesized six Pxt-related peptides (Pxt-2, Pxt-5, Pxt-12, reverse Pxt-2, reverse Pxt-5 and reverse Pxt-12) and three amphiphilic α-helical peptides (magainin 1, mastoparan and melittin) (*20*–*22*), as control peptides (Table I). The reason for selecting the three Pxt peptides Pxt-2, Pxt-5 and Pxt-12 was that they all exhibited significant foaming activities in the course of peptide synthesis. The magainin 1 and mastoparan were selected as representative AMPs, while melittin is a well-known hemolytic peptide.

The Schiffer–Edmundson helical wheel projections of Pxt-related peptides and control peptides by GPMAW10.0 software (http://www.GPMAW.com) are shown in Fig. 1A and B. In all the peptides studied, the hydrophilic amino acids, such as asparagine, arginine and lysine, were localized at one face, while hydrophobic amino acids, such as isoleucine, leucine and phenylalanine, were at the other face. Moreover, the grand average of hydropathy (GRAVY) values for the peptides were calculated by the same software; the GRAVY value is defined by the sum of hydropathy values of all amino acids divided by the protein length. A positive GRAVY value indicates a hydrophobic feature, whereas a negative means hydrophilic one (*23*). The GRAVY values of Pxt-related peptides (Pxt-2, Pxt-5, Pxt-12, reverse Pxt-2, reverse Pxt-5 and reverse Pxt-12) and the control peptides (magainin 1, mastoparan and melittin) were positive (0.2–1.6) and comparatively higher among Pxt peptides, as shown in Table I. These data suggest that all the tested peptides had the possibility to form an amphiphilic α-helix. Therefore, we measured CD spectra of these peptides in aqueous buffer (10 mM Tris–HCl, pH 7.2) and organic solvent (50% TFE), since TFE is well-known to facilitate the formation of secondary structure, such as an α-helix in membrane-mimetic environments (*24*). As shown in Table II, when the CD spectra of these peptides were measured in aqueous buffer, Pxt-5, reverse Pxt-5, mastoparan and melittin exhibited representative α-helical structures. In the 50% TFE solvent, all Pxt-related peptides and control peptides formed significant amphiphilic α-helix in the more hydrophobic environments.

Next, we measured the surface tensions of these peptides using the pendant drop method at 25°C. Surface tension of water at 25°C is reported to be 71.99 mN/m (*25*). As shown in Fig. 2A and B, all Pxt-related peptides and control peptides decreased their surface tensions in a concentration-dependent manner. Among Pxt-related peptides, both Pxt-5 and reverse Pxt-5 were the most effective to reduce their surface tensions to the level of about 38 mN/m. Pxt-12 and reverse Pxt-12 did not reduce their surface tensions better than Pxt-5 and reverse Pxt-5. On the other hand, the control peptides (magainin 1, mastoparan and melittin) gradually decreased their surface tensions, while Pxt-2, Pxt-5 and reverse Pxt-5 had constant surface tensions above their critical association concentrations between $10^{-6}$and 10^{-5}M, suggesting the formation of micelle-like assemblies.

Table I. Amino acid sequences of Pxt-related peptides from *Xenopus tropicalis* skin and GRAVY

Peptide	Sequence	Monoisotopic mass	GRAVY value	Number of cationic amino acids
Pxt-1	IRPIPFIPRGGKT-NH_2	1,449.8	−0.223	
Pxt-2	**FIGALL[R]PAL[K]LLA-NH2**	**1,493.9**	**1.521**	2
Pxt-3	GLKEVAHSAKKFAKGFISGLTGS	2,332.2	0.013	
Pxt-4	LKGASKLIPHLLPSRQQ	1,885.1	−0.365	
Pxt-5	**FIGALLGPLLNLL[K]-NH2**	**1,479.9**	**1.579**	1
Pxt-6	IRPVPFFPPVHAKKVFPLH	2,225.2	0.232	
Pxt-7	Pyr-GLIGTLTAKQIKK-NH_2	1,479.9	0.077	
Pxt-8	IRPIPFIPR	1,107.6	0.278	
Pxt-9	GLKEVAHSAKKF	1,313.7	−0.433	
Pxt-10	LMGTLISKQMKK-NH_2	1,375.8	−0.100	
Pxt-11	Pyr-GLMGTLISKQMKK-NH_2	1,543.8	−0.123	
Pxt-12	**NLLGSLL[K]TGL[K]VGSNLL-NH2**	**1,839.1**	**0.694**	2
Reverse Pxt-2	**ALL[K]LAP[R]LLAGIF-NH2**	**1,493.9**	**1.521**	2
Reverse Pxt-5	**[K]LLNLLPGLLAGIF-NH2**	**1,479.9**	**1.579**	1
Reverse Pxt-12	**LLNSGV[K]LGT[K]LLSGLLN-NH2**	**1,839.1**	**0.694**	2
Magainin 1	**GIG[K]FL[H]SAG[K]FG[K]AFVG*E*IM[K]S**	**2,408.3**	**0.217**	5
Mastoparan	**INL[K]ALAALA[KK]IL-NH2**	**1,478.0**	**1.157**	3
Melittin	**GIGAVL[K]VLTTGLPALISWI[KRKR]QQ-NH2**	**2,844.8**	**0.273**	5

GRAVY values of Pxt peptides were calculated by GPMAW10.0 software (http://www.GPMAW.com), according to the method of Kyte and Doolittle (*25*). Cationic and anionic amino acids were indicated as boxed and italic letters, respectively. Underline showed the sequence similarity. Boxed letters were indicated as different amino acids from those of Pxt peptides.

Biological properties of Pxt-related peptides

We previously reported antimicrobial activities and hemolytic activities of Pxt peptides using Gram-negative bacterium (*E.coli*), Gram-positive bacterium (*St.aureus*) and heparinized rat whole blood (*10*). But, to further characterize the biological properties of Pxt-related peptides (Pxt-2, Pxt-5, Pxt-12, reverse Pxt-2, reverse Pxt-5 and reverse Pxt-12) and control peptides (magainin 1, mastoparan and melittin), we utilized Gram-negative bacteria (*E.coli* and *P.aeruginosa*), Gram-positive bacteria (*St.aureus* and *M.luteus*), yeasts (*Sa. cerevisiae* and *C.albicans*), heparinized rat whole blood and rat peritoneal mast cells for antimicrobial, hemolytic and histamine-releasing activities of Pxt-related peptides, respectively. As references peptides, magainin 1, mastoparan and melittin were selected for the antimicrobial, histamine-releasing and hemolytic assays, respectively.

Antimicrobial activities of Pxt-related peptides

As shown in Table III, with the exception of reverse Pxt-12, Pxt-related peptides (Pxt-2, Pxt-5, Pxt-12, reverse Pxt-2 and reverse Pxt-5) exhibited the antimicrobial activities with MIC values for both Gram-negative (*E.coli* and *P.aeruginosa*) and Gram-positive bacteria (*St.aureus* and *M.luteus*) of less than 12.5, 25 or 50 μM; this was also true of magainin 1. In the case of yeasts, Pxt-5, Pxt-12, reverse Pxt-2, reverse Pxt-5 and magainin 1 only exhibited the significant growth inhibitory effects on *Sa. cerevisiae*, while none of the tested peptides could affect the growth of *C.albicans*. Some of the antimicrobial activities in our study were slightly different from those previously reported (*10*), because of the different assay conditions, including different bacteria strains.

Hemolytic activities of Pxt-related peptides

Next, we examined the hemolytic activities of Pxt-related peptides using rat whole blood. As shown in Table III, among Pxt-related peptides, the Pxt-5 peptide (5×10^{-5} M) displayed the highest hemolytic activity (69.8% hemolysis), while Pxt-2, reverse Pxt-2, reverse Pxt-5 and mastoparan at 50 μM showed only 2.0, 1.5, 5.2 and 13.5% hemolysis, respectively. Mellitin, the lytic and toxic component of bee venom (*26*), showed 100% complete hemolysis at 10^{-5} M, while Pxt-12 and reverse Pxt-12 did not display any hemolytic activity at 5×10^{-5} M.

Histamine-releasing activities of Pxt-related peptides

Rat peritoneal mast cells are known to secrete histamine when stimulated by both IgE with multivalent antigens and various amphiphilic substances, including mastoparan (*27*). All Pxt-related peptides induced a significant and dose-dependent histamine release. As shown in Table III, they all exhibited about 20–50% of the total cellular histamine release at 10^{-5} M, as did mastoparan and melittin.

Cytotoxic effects of Pxt-related peptides on human keratinocyte HaCaT cells

HaCaT cells, spontaneously immortalized human keratinocyte cells (*28*), have been widely used as a skin exposure model. To examine the cytotoxic effects of Pxt-related peptides on HaCaT cells, the mitochondrial activity and the cellular membrane injury were measured by the MTT assay and LDH assay, respectively.

HaCaT cells were exposed to Pxt-related peptides (10^{-5} to 10^{-3} M) and the cell viability was measured after 6 and 24 h of exposure using the MTT assay. As shown in Fig. 3A and B, all Pxt-related peptides, magainin 1 and mastoparan dose dependently inhibited cell viability after 6 or 24 h exposures. After 24 h exposure, Pxt-12, reverse Pxt-2 and reverse Pxt-5, as well as magainin 1 and mastoparan, did not significantly affect the cell viability at 10^{-5} M. Among Pxt-related peptides, Pxt-5 displayed the much more potent cytotoxic effects. On the other hand, melittin

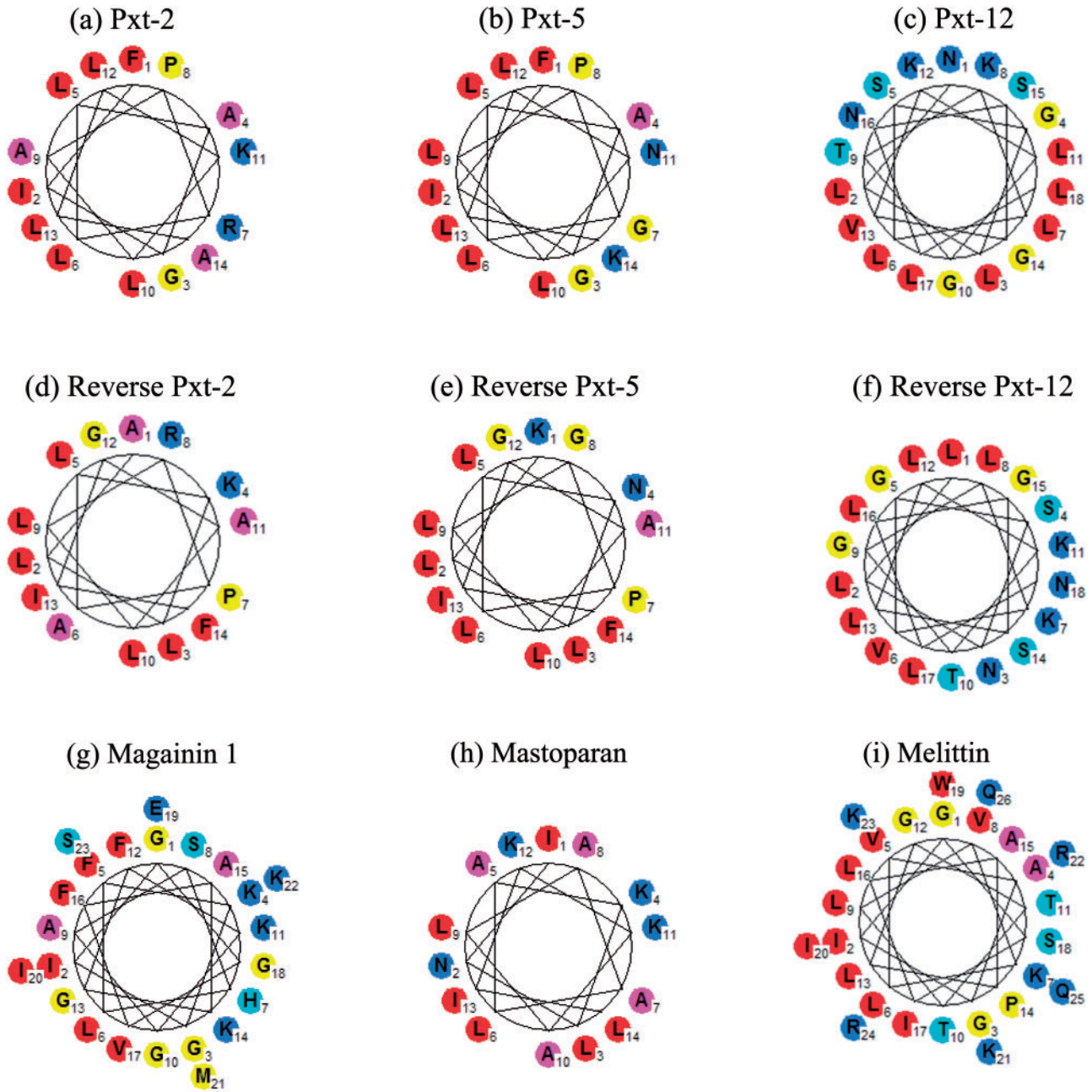

Fig. 1 (A, B) Schiffer–Edmundson helical wheel representations of Pxt-related peptides. Pxt-2 (a), Pxt-5 (b), Pxt-12 (c), reverse Pxt-2 (d), reverse Pxt-5 (e), reverse Pxt-12 (f), magainin 1 (g), mastoparan (h), and melittin (i). Amino acids were shown as follows: blue [Glu (E), Asp (D), Gln (Q), Asn (N), Lys (K), Arg (R)], cyan [Ser (S), Thr (T), His (H)], yellow [Gly (G), Met (M), Pro (P), Cys (C)], magenta [Ala (A)] and red [Val (V), Leu (L), Ile (I), Trp (W), Tyr (Y), Phe (F)]. Data of Pxt-2 (a), Pxt-5 (b), reverse Pxt-5 (e), magainin 1 (g) and mastoparan (h) were reported in our previous paper (*10*).

Table II. Helical contents of Pxt-related peptides by CD measurements

	Helical content (%) in 10 mM Tris–HCl (pH 7.2)			Helical content (%) in 50% TFE		
Peptide	**10°C**	**25°C**	**37°C**	**10°C**	**25°C**	**37°C**
Pxt-2	2.5	3.5	5.7	22.1	19.7	18.7
Pxt-5	59.8	62.0	64.6	51.0	48.0	45.2
Pxt-12	0	2.5	6.6	68.2	57.4	50.5
Reverse Pxt-2	3.6	4.7	7.3	28.6	26.8	22.8
Reverse Pxt-5	10.9	17.4	19.8	87.1	77.0	70.7
Reverse Pxt-12	0	0	2.0	23.7	21.0	17.9
Magainin 1	0	0.3	2.3	100	100	84.0
Mastoparan	24.7	23.5	25.7	95.8	90.2	86.2
Melittin	9.2	11.2	13.9	77.2	74.6	71.5

All peptides were analysed in 10 mM Tris–HCl (pH 7.2) or 50% TFE at 10, 25 and 37°C. The α-helical contents of the peptides were calculated by the method of Forood *et al.* (*11*).

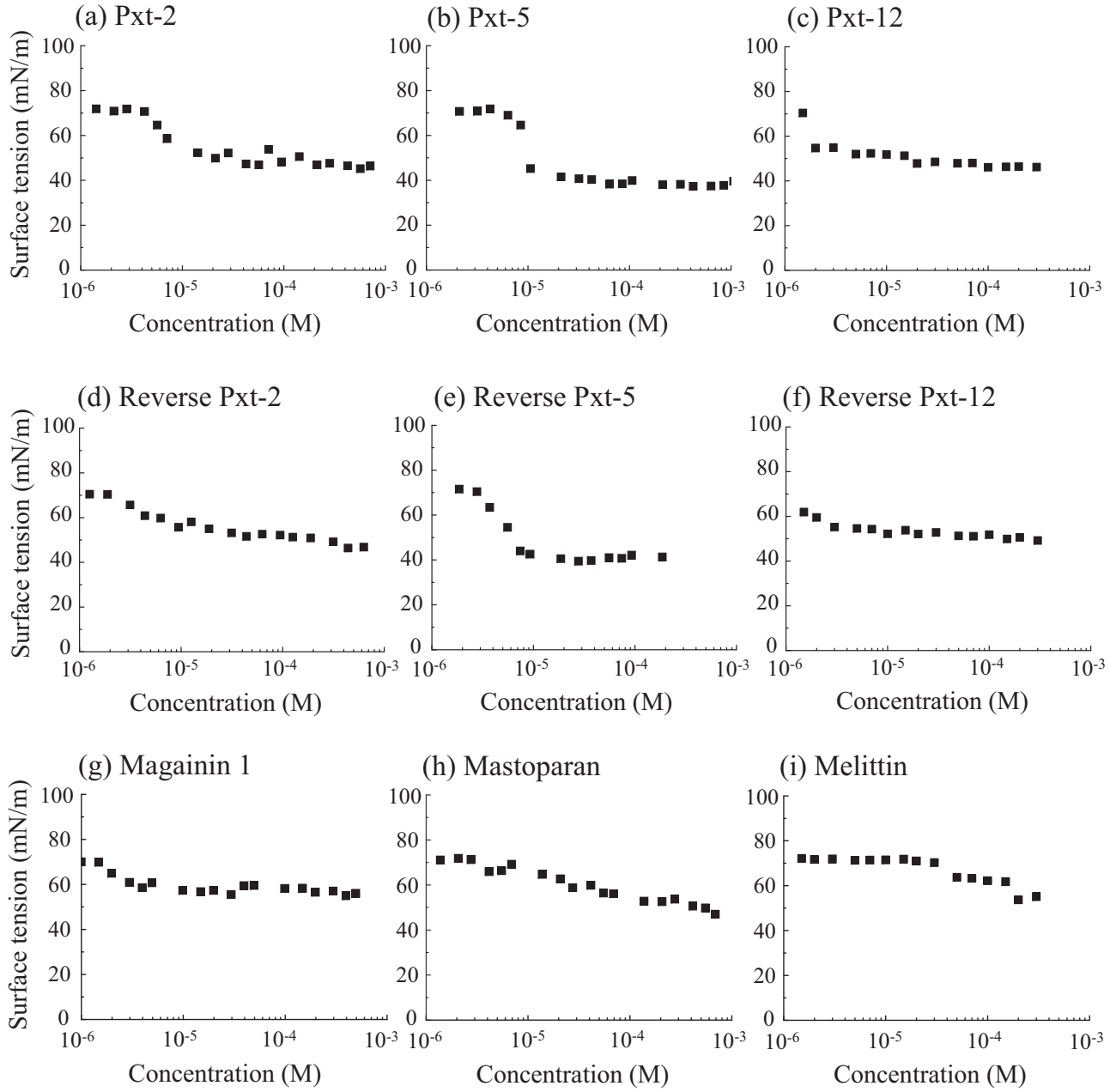

Fig. 2 (A, B) Surface tension of Pxt peptide solutions. Pxt-2 (a), Pxt-5 (b), Pxt-12 (c), reverse Pxt-2 (d), reverse Pxt-5 (e), reverse Pxt-12 (f), magainin 1 (g), mastoparan (h) and melittin (i). The surface tensions of Pxt peptide solutions were determined by the pendant drop method at 25°C. Data of Pxt-2 (a), Pxt-5 (b), reverse Pxt-5 (e), magainin 1 (g) and mastoparan (h) were reported in our previous paper (*10*).

Table III. Biological properties of Pxt-related peptides

	MIC							
Peptide	***Escherichia coli* (μM)**	***Pseudomonas aeruginosa* (μM)**	***Saphylococcus aureus* (μM)**	***Micrococcus luteus* (μM)**	***Saccharomyces cerevisiae* (μM)**	***Candida albicans* (μM)**	**Hemolytic activity (at 50 μm)**	**Histamine release (at 10 μm)**
Pxt-2	<12.5	<50	<12.5	<25	ND	ND	2.0%	22.8%
Pxt-5	<50	<50	<12.5	<12.5	Significant	ND	69.8%	32.8%
Pxt-12	<12.5	<50	<12.5	<50	Significant	ND	0%	25.6%
Reverse Pxt-2	<12.5	<50	<12.5	<50	Significant	ND	1.5%	50.4%
Reverse Pxt-5	<12.5	<50	<12.5	<25	Significant	ND	5.2%	46.5%
Reverse Pxt-12	ND	ND	ND	ND	ND	ND	0%	25.6%
Magainin 1	<12.5	<25	<25	Significant	<50	ND	–	–
Mastoparan	–	–	–	–	–	–	13.5%	31.1%
Melittin[a]	–	–	–	–	–	–	100%	64.3%

ND, not detected; –, determined; significant, bacterial growth was suppressed in the presence of peptides.
[a]Hemolytic activity of melittin at 10 μM was indicated.

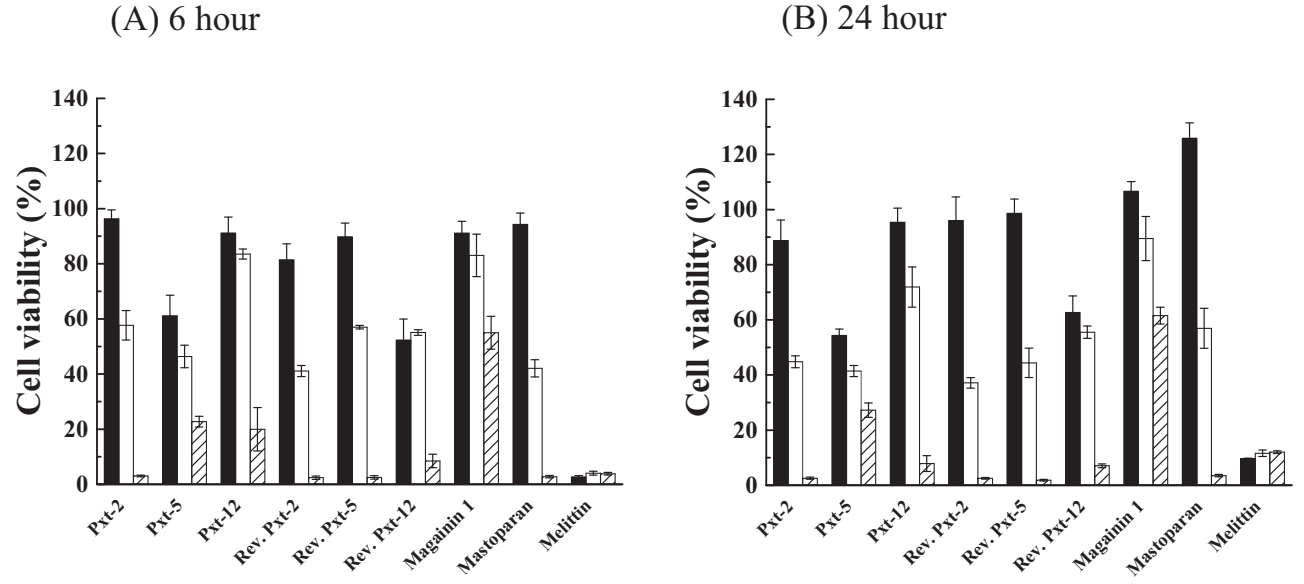

Fig. 3 MTT assays in cultured HaCaT cells, treated with Pxt-related peptides and control peptides (magainin 1, mastoparan and melittin) (10^{-5} to 10^{-3} M) for 6 h (A) or 24 h (B). Black, white and shade bars showed 10^{-5}, 10^{-4} and 10^{-3} M peptide treatments, respectively.

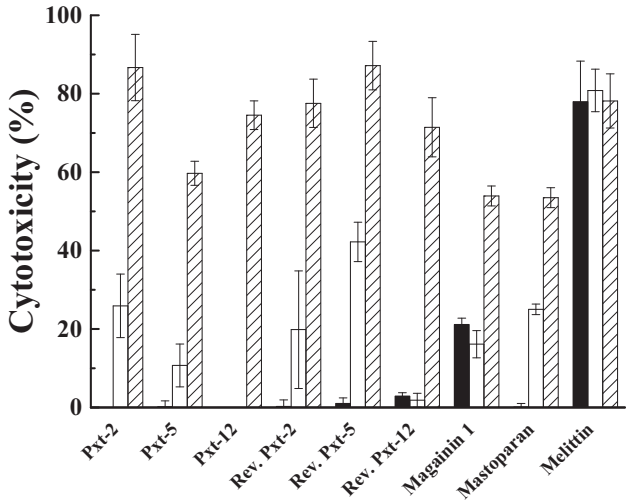

Fig. 4 LDH assays in cultured HaCaT cells, treated with Pxt-related peptides and control peptides (magainin 1, mastoparan and melittin) (10^{-5} to 10^{-3} M). Black, white and shade bars showed 10^{-5}, 10^{-4} and 10^{-3} M peptide treatments, respectively.

at a concentration of 10^{-5} M, severely suppressed the cell viability of HaCaT cells to $2.6 \pm 0.4\%$ (mean ± standard deviation [SD]), even after only 6 h exposure.

LDH, a soluble cytoplasmic enzyme, is released into extracellular space when the plasma membrane is damaged. We examined the cytotoxic effects of Pxt-related peptides on HaCaT cells by the measurement of released LDH. In addition to the MTT assay, HaCaT cells were exposed to Pxt-related peptides (10^{-5} to 10^{-3} M) for 24 h. As shown in Fig. 4, all Pxt-related peptides induced LDH release into the medium in a dose-dependent manner, as did magainin 1 and mastoparan. Among Pxt-related peptides, Pxt-12 exhibited the weakest LDH release, while melittin, even at 10^{-5} M, exhibited potent LDH release ($77.9 \pm 10.3\%$, mean ± SD).

Inflammatory effects of Pxt-related peptides on human keratinocyte HaCaT cells

IL-8 (CXCL8), a member of the CXC chemokine family, is often associated with inflammation (*29*). HaCaT cells are known to produce IL-8 as part of their inflammatory response, while they normally secrete a very low amount of IL-8 (*30*). This IL-8 synthesis is known to be controlled at transcriptional or post-transcriptional levels. To examine the inflammatory effects of Pxt-related peptides on HaCaT cells, HaCaT cells were exposed to Pxt-related peptides (10^{-4} M for gene expression and 10^{-5} to 10^{-3} M for secreted IL-8) for 24 h. Gene expression and secreted IL-8 levels were measured by RT-PCR and ELISA, respectively. With respect to the gene expression of IL-8 in response to Pxt-related peptide exposure, reverse Pxt-2 and reverse Pxt-5 were the most potent, providing 3.8 - and 12.2-fold higher levels of expression than the basal IL-8 gene expression level, respectively, as shown in Fig. 5A. In the case of melittin, the IL-8 gene expression level could not be measured due to the tested cells dying. In ELISA experiments, as well as in the gene expression experiment, reverse Pxt-2 and reverse Pxt-5 at 10^{-4} M were the most potent stimulators of IL-8 secretion among the tested Pxt-related peptides, with extracellular levels reaching 685.5 and 554.5 pg/ml. The basal level of secreted IL-8 was 120.4 ± 20.7 pg/ml (mean ± SD). At 10^{-3} M concentration, with the exception of Pxt-12 and reverse Pxt-12, IL-8 secretion stimulated by Pxt-related peptides was reduced, compared to the responses at 10^{-5} or 10^{-4} M Pxt-related peptides. Taking into consideration the MTT and LDH data, cell death in HaCaT cells seemed to occur after the treatment with higher

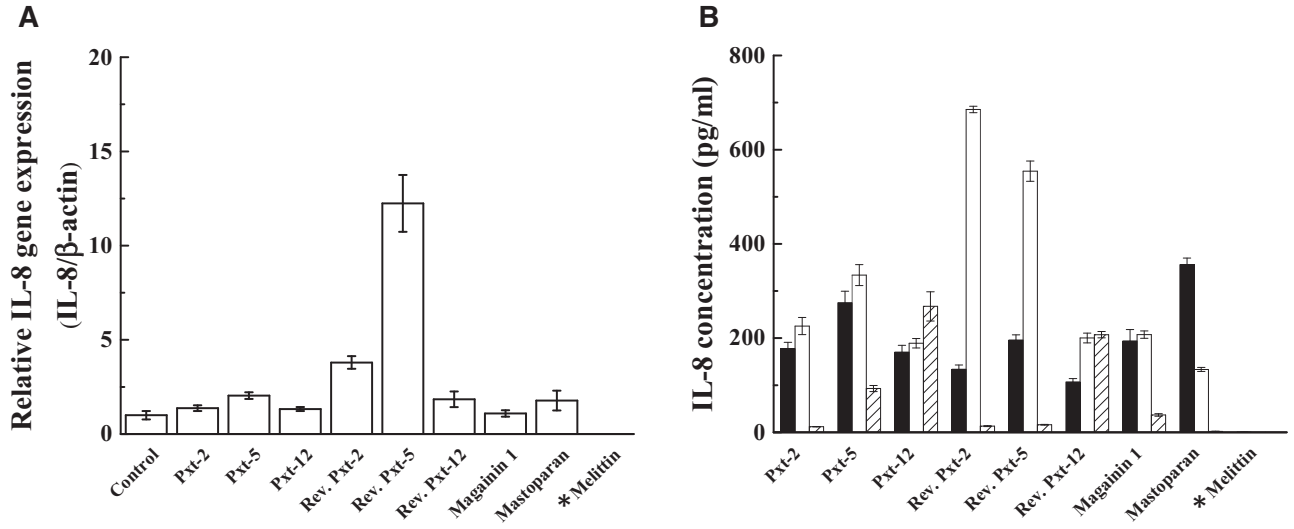

Fig. 5 The mRNA transcript level of IL-8 in cultured HaCaT cells, a skin exposure model, treated with Pxt-related peptides and control peptides (magainin 1, mastoparan and melittin) (10^{-4} M) (A). The secretory level of IL-8 in cultured HaCaT cells, treated with Pxt-related peptides and control peptides (magainin 1, mastoparan and melittin) (10^{-5} to 10^{-3} M) (**B**). IL-8 concentration was determined by ELISA. Black, white and shade bars showed 10^{-5}, 10^{-4} and 10^{-3} M peptide treatments, respectively. *In the case of melittin, IL-8 measurements could not be done due to the death of HaCaT cells.

concentrations of Pxt-related peptide (10^{-3} M) and control peptides (magainin 1 and mastoparan).

Effects of Pxt-related peptides on oxidative stress response in human keratinocyte HaCaT cells

HMOX is the rate-limiting enzyme that catalyzes the degradation of heme and yields biliverdin, iron and carbon monoxide as the final products (*31*). Among three isoforms of HMOX, HMOX-1 is an inducible isoform in response to stress, such as oxidative stress, hypoxia and so on. To examine the effects of Pxt-related peptides on the oxidative stress response in HaCaT cells, the gene expression level of HMOX-1 was measured by RT-PCR after the exposure of Pxt-related peptides (10^{-4} M) for 24 h. As shown in Fig. 6, all Pxt-related peptides, with the exception of reverse Pxt-5, had few effects on HMOX-1 gene expression, as was also the case for magainin 1. In contrast, reverse Pxt-5 and mastoparan induced 98.6- and 37.3-fold higher gene expression levels of HMOX-1 than basal one, respectively. In the case of melittin, the tested cells died and mRNA was not recovered.

Homology search and gene expression of Pxt peptides in Xenopus tropicalis

In order to search for clues about possible physiological roles of Pxt peptides (Pxt-1 through Pxt-12) *in vivo*, we performed the amino acid homology search using NCBI BLAST. Although some homologous sequences to Pxt peptides were presented from different biological species, as shown in Table IV, we could not uncover the important key to solve their physiological functions. Next, we examined the gene expression of Pxt-2, Pxt-5 and Pxt-12 by RT-PCR using total RNA extracted from different *X.tropicalis* tissues (testis, ovary, skin, brain, heart, kidney, muscle, spleen, lung, stomach, intestine, liver and pancreas). EF1 α, an essential component of the eukaryotic translational apparatus, was utilized as an internal standard. As shown in Fig. 7, Pxt-2 was only detected in *X.tropicalis* skin. In contrast, in addition to *X.tropicalis* skin, Pxt-5 and Pxt-12 were detected in testis and muscle, respectively.

Discussion

In this study, we further performed the physicochemical and biological characterizations of Pxt peptides after the discovery of Pxt peptides from the skin of the amphibian *X.tropicalis* using direct tissue MALDI-MS analysis (*10*). The Schiffer–Edmundson helical wheel projections and CD measurements demonstrated that Pxt-5 and reverse Pxt-5 could form α-helical structures in both aqueous buffer and organic solvent, while α-helical formation of Pxt-2, Pxt-12, reverse Pxt-2 and reverse Pxt-12 were facilitated in organic solvent, membrane-mimetic environments.

Among Pxt-related peptides, Pxt-5 showed the most potent hemolytic activity and much more potent cytotoxicity on HaCaT cells in the MTT assay. On the other hand, reverse Pxt-5 showed the most remarkable gene expression of IL-8 and HMOX-1 in HaCaT cells and the most potent cytotoxicity of LDH release among Pxt-related peptides. As shown in Fig 2, Pxt-5 and reverse Pxt-5 possessed the strongest capacity character to reduce their surface tensions and behaved like micelle assemblies at more than 10^{-5} M. In addition to being better at forming α-helical structures in both aqueous buffer and organic solvent, the detergent-like action of Pxt-5 and reverse Pxt-5 might be effective in facilitating these potent biological characteristics.

In antimicrobial, hemolytic, cell viability and cytotoxicity assays in HaCaT cells, Pxt-12 and reverse Pxt-12 were the weakest among Pxt-related peptides.

Similar results for CPF-St7, identical to Pxt-12, were reported by Roelants *et al*. (*9*). The antimicrobial mechanism of these α-helical peptides has been proposed as being an interaction with negatively charged phospholipids and the spontaneous formation of membrane spanning pores that permit peptide translocation to the inner leaflet upon disintegration of the pore (*32*, *33*). Pxt-12 and reverse Pxt-12 have only two cationic amino acids and exhibited lower helical content in organic solvent (50% TFE), compared to magainin 1 (Tables I and II). These physicochemical characteristics of Pxt-12 and reverse Pxt-12 seemed to be the reasons in part for their weak biological activities.

We synthesized three Pxt pepides (Pxt-2, Pxt-5 and Pxt-12) and three reverse peptides (reverse Pxt-2, reverse Pxt-5 and reverse Pxt-12). Although three pairs of peptides (Pxt-2 and reverse Pxt-2, Pxt-5 and reverse Pxt-5, and Pxt-12 and reverse Pxt-12) have the same amino acid composition and similar amphiphilicity (Fig. 1), they exhibited different properties in the physicochemical and biological experiments. For example, α-helical contents in both aqueous buffer and organic solvent were not similar within two sets (Pxt-5 and reverse Pxt-5, and Pxt-12 and reverse Pxt-12). In the antimicrobial experiment, reverse Pxt-12 was the only one of these synthesized Pxt peptides that had no antimicrobial effects on any microorganisms. Pxt-5 showed much more potent effects in the MTT assay in HaCaT cell cytotoxicity than reverse Pxt-5. IL-8 expression in gene and protein levels was the most strongly induced by the exposure of the cells to reverse Pxt-2 and reverse Pxt-5. Moreover, the most potent induction of HMOX-1, a marker of oxidative stress response, was observed with exposure to reverse Pxt-5, but not Pxt-5. We do not know the explanation for the diversity of the phenomena described above, but subtle, different properties of Pxt-related peptides, such as their polarity, might affect and determine their various activities. Further studies should be required to clarify the above phenomena in detail and we are planning their structural analysis using nuclear magnetic resonance or X-ray crystallography.

In *X.laevis*, magainin 1, magainin 2, PGLa (a peptide with amino-terminal glycine and carboxy-terminal leucine amide), caerulein precursor factor, xenopsin precursor factor and pGQ (a peptide with amino-terminal glycine and carboxy-terminal glutamine) were detected in extracts of stomach tissue (*34*). Magainin and PGLa mRNAs were highly detected throughout the entire gastrointestinal tract in *X.laevis*, such as stomach, duodenum, distal small intestine and large intestine/colon, as well as in skin (*35*). Additionally, *in situ* hybridization experiments showed

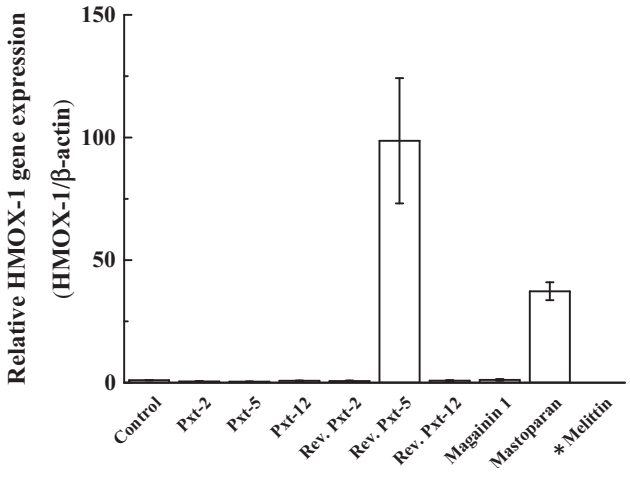

Fig. 6 The mRNA transcript level of HMOX-1, a marker of oxidative stress, in cultured HaCaT cells, treated with Pxt-related peptides and control peptides (magainin 1, mastoparan and melittin) (10^{-4} M). *In the case of melittin, HMOX-1 measurement could not be done due to the death of HaCaT cells.

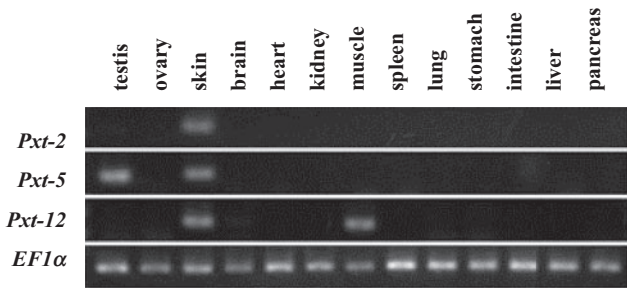

Fig. 7 RT-PCR analysis of mRNA expression of Pxt peptides (Pxt-2, Pxt-5 and Pxt-12) in *Xenopus tropicalis* tissue (testis, ovary, skin, brain, heart, kidney, muscle, spleen, lung, stomach, intestine, liver and pancreas). EF1 α was utilized as an internal standard.

Table IV. Amino acid sequences with higher homology to Pxt peptides using BLAST search

		Amino acid sequences (name of proteins, biological species)
Pxt-1	IRPIPFIPRGGKT-NH_2	IPFIPRGGK (3-isopropylmalate dehydratase, *Paenibacillus popilliae*)
Pxt-2	FIGALLRPALKLLA-NH_2	ALLRSALKLLA (phospho protein phosphatase-like protein, *Emiliania huxleyi* CCMP1516)
Pxt-3	GLKEVAHSAKKFAKGFISGLTGS	KQVAHEAKKFAK (StbA family protein, *Vibrio* sp. CAIM 1540)
Pxt-4	LKGASKLIPHLLPSRQQ	LKFASKLITHLLQNRQQ (thyroid adenoma-associated protein, *Opisthocomus hoazin*)
Pxt-5	FIGALLGPLLNLLK-NH_2	FFGALLGALLNYLLK (hypothetical protein, *Vibrio harveyi*)
Pxt-6	IRPVPFFPPVHAKKVFPLH	PFFPSIHAKGVFP (bone morphogenetic protein 7, *Anas platyrhynchos*)
Pxt-7	Pyr-GLIGTLTAKQIKK-NH_2	MIGTMTAKQIK (5′-nucleotidase, *Tumebacillus flagellates*)
Pxt-8	IRPIPFIPR	IKPVPFIPR (enoyl reductase domain of FAS1, *Aspergillus oryzae* 3.042)
Pxt-9	GLKEVAHSAKKF	EVAHSAKKF (hypothetical protein M569_06888, *Genlisea aurea*)
Pxt-10	LMGTLISKQMKK-NH_2	MGLETLIASKQMKK (peptidase M13, *Pedobacter* sp. V48)
Pxt-11	Pyr-GLMGTLISKQMKK-NH_2	GLMLAMELATLTSKQMKK (NADH dehydrogenase subunit 5, *Synodus variegatus*)
Pxt-12	NLLGSLLKTGLKVGSNLL-NH_2	LLKTGLKVGSKL (glycosyltransferase, *Halococcus thailandensis*)

Underline showed the sequence similarity. Boxed letters were indicated as different amino acids from those of Pxt peptides.

that magainin and PGLa mRNAs were synthesized in the granular multinucleated cells of the gastric mucosa and Paneth-like cells in the small intestine of *X.laevis*. These results raised the possibility of their involvement in intestinal host defense systems, gene duplication of AMPs and a shift in gene expression of AMPs from the gastrointestinal tract and brain to the granular skin glands (*9*). In the case of Pxt peptides (Pxt-2, Pxt-5 and Pxt-12), gene expression of Pxt-2 was only detected in skin, as shown in Fig. 7. Although the Pxt-5 and Pxt-12 genes were expressed in testis and muscle, respectively, as well as skin, gene expression of all three Pxt peptides was not detected in stomach, intestine, liver or pancreas at all. Taken together, the evolutionary mechanism of Pxt-peptides (Pxt-2, Pxt-5 and Pxt-12) might be different from those of magainin and PGLa in *X.laevis*.

Acknowledgements

We are grateful to Prof. Leslie Sargent Jones (Appalachian State University) for her careful reading of our manuscript and Dr Akikazu Yasuda for his valuable comments.

Funding

This work was supported by JSPS KAKENHI Grant Number15K01814, Sekisui Chemical Innovations inspired by nature research support program and an AIST research grant.

Conflict of Interest

None declared.

References

1. Conlon, M. (2011) The contribution of skin antimicrobial peptides to the system of innate immunity in anurans. *Cell Tissue Res*. **343**, 201–212
2. Morikawa, N., Hagiwara, K., and Nakajima, T. (1992) Brevinin-1 and -2, unique antimicrobial peptides from the skin of the frog, *Rana brevipoda porsa*. *Biochem. Biophys. Res. Commun*. **189**, 184–190
3. Mor, A., Nguyen, V., Delfour, A., Migliore-Samour, D., and Nicolas, P. (1991) Isolation, amino acid sequence, and synthesis of dermaseptin, a novel antimicrobial peptide of amphibian skin. *Biochemistry* **30**, 8824–8830
4. Zasloff, M. (2002) Antimicrobial peptides of multicellular organisms. *Nature* **415**, 389–395
5. Wang, G., Li, X., and Wang, Z. (2009) APD2: the updated antimicrobial peptide database and its application in peptide design. *Nucleic Acid Res*. **37**, D933–D937
6. Konig, E., Bininda-Emonds, O., and Shaw, C. (2015) The diversity and evolution of anuran skin peptides. *Peptides* **63**, 96–117
7. Hellsten, U., Harland, R., Gilchrist, M., Hendrix, D., Jurka, J., Kapitonov, V., Ovcharenko, I., Putnam, N., Shu, S., Taher, L., Blitz, I., Blumberg, B., Dichmann, D., Dubchak, I., Amaya, E., Detter, J., Fletcher, R., Gerhard, D., Goodstein, D., Graves, T., Grigoriev, I., Grimwood, J., Kawashima, T., Lindquist, E., Lucas, S., Mead, P., Mitros, T., Ogino, H., Ohta, Y., Poliakov, A., Pollet, N., Robert, J., Salamov, A., Sater, A., Schmutz, J., Terry, A., Vize, P., Warren, W., Well, D., Wills, A., Wilson, R., Zimmerman, L., Zorn, A., Grainger, R., Grammer, T., Khokha, M., Richardson, P., and Rokhsar, D. (2010) The genome of the Western clawed frog *Xenopus tropicalis*. *Science* **328**, 633–636
8. Ali, M., Soto, A., Knoop, F., and Conlon, M. (2001) Antimicrobial peptides isolated from skin secretions of the diploid frog, *Xenopus tropicalis* (Pipidae). *Biochim. Biophys. Acta* **1550**, 81–89
9. Roelants, K., Fry, B., Ye, L., Stijlemans, B., Brys, L., Kok, P., Clynen, E., Schoofs, L., Cornelis, P., and Bossuyt, F. (2013) Origin and functional diversification of an amphibian defense peptide arsenal. *PLoS Genet*. **9**, e1003662
10. Shigeri, Y., Yasuda, A., Hagihara, Y., Nishi, K., Watanabe, K., Imura, T., Inagaki, H., Haramoto, Y., Ito, Y., and Asashima, M. (2015) Identification of novel peptides from amphibian (*Xenopus tropicalis*) skin by direct tissue MALDI-MS analysis. *FEBS J*. **282**, 102–113
11. Forood, B., Feliciano, E., and Nambiar, K. (1993) Stabilization of alpha-helical structures in short peptides via end capping. *Proc. Natl. Acad. Sci. U S A*. **90**, 838–842
12. Imura, T., Tsukui, Y., Taira, T., Aburai, K., Sakai, K., Sakai, H., Abe, M., and Kitamoto, D. (2014) Surfactant-like properties of an amphiphilic alpha-helical peptide leading to lipid nanodisc formation. *Langmuir* **30**, 4752–4759
13. Steinberg, D. and Lehrer, R. (1997) Designer assays for antimicrobial peptides. Disputing the ''one-size-fits-all'' theory. *Methods Mol. Biol*. **78**, 169–186
14. Inagaki, H., Akagi, M., Imai, H., Taylor, R., and Kubo, T. (2004) Molecular cloning and biological characterization of novel antimicrobial peptides, pilosulin 3 and pilosulin 4, from a species of the Australian ant genus *Myrmecia*. *Arch. Biochem. Biophys*. **428**, 170–178
15. Inagaki, H., Akagi, M., Imai, H., Taylor, R., Weise, M., Davies, N., and Kubo, T. (2008) Pilosulin 5, a novel histamine-releasing peptide of the Australian ant, *Myrmecia pilosula* (Jack Jumper Ant). *Arch. Biochem. Biophys*. **477**, 411–416
16. Akagi, M., Mio, K., Miyoshi, K., and Tasaka, K. (1987) Antiallergic effects of terfenadine on immediate type hypersensitivity reactions. *Immunopharmacol. Immunotoxicol*. **9**, 257–279
17. Horie, M., Stowe, M., Tabei, M., Kato, H., Nakamura, A., Endoh, S., Morimoto, Y., and Fujita, K. (2013) Dispersant affects the cellular influences of single-wall carbon nanotube: the role of CNT as carrier of dispersants. *Toxicol. Mech. Methods* **23**, 315–322
18. Tabei, Y., Sonoda, A., Nakajima, Y., Biju, V., Makita, Y., Yoshida, Y., and Horie, M. (2015) In vitro evaluation of the cellular effect of indium tin oxide nanoparticles using the human lung adenocarcinoma A549 cells. *Metallomics* **7**, 816–827
19. Roelants, K., Fry, B., Norman, J., Clynen, E., Schoofs, L., and Bossuyt, F. (2010) Identical skin toxins by convergent molecular adaptation in frogs. *Curr. Biol*. **20**, 125–130
20. Matsuzaki, K. (1998) Magainins as paradigm for the mode of action of pore forming polypeptides. *Biochim. Biophys. Acta* **1376**, 391–400
21. Hirai, Y., Yasuhara, T., Yoshida, H., Nakajima, T., Fujino, M., and Kitada, C. (1979) A new mast cell degranulating peptide ''mastoparan'' in the venom of *Vespula lewisii*. *Chem. Pharm. Bull*. **27**, 1942–1944
22. Habermann, E. (1972) Bee and wasp venoms. *Science* **177**, 314–322

23. Kyte, J. and Doolittle, R. (1982) A simple method for displaying the hydropathic character of a protein. *J. Mol. Biol.* **157**, 105–132
24. Kallenbach, N., Lyu, P., and Zhou, H. (1996) Circular Dichroism and the Conformational Analysis of Biomolecules. (Fasman G.D., ed.) pp. 201–269, Plenum Press, New York
25. Vargaftik, N., Volkov, B., and Voljak, L. (1983) International tables of the surface tension of water. *J. Phys. Chem. Ref. Data* **12**, 817–820
26. Terwilliger, T. and Eisenberg, D. (1982) The structure of melittin. II. Interpretation of the structure. *J. Biol. Chem.* **257**, 6016–6022
27. Lagunoff, D., Martin, T., and Read, G. (1983) Agents that release histamine from mast cells. *Annu. Rev. Pharmacol. Toxicol.* **23**, 331–351
28. Boukamp, P., Petrussevska, R., Breitkreutz, D., Hornung, J., Markham, A., and Fusenig, N. (1988) Normal keratinization in a spontaneously immortalized aneuploid human keratinocyte cell line. *J. Cell. Biol.* **106**, 761–771
29. White, G., Iqbal, A., and Greaves, D. (2013) CC chemokine receptors and chronic inflammation—therapeutic opportunities and pharmacological challenges. *Pharmacol. Rev.* **65**, 47–89
30. Raingeaud, J. and Pierre, J. (2005) Interleukin-4 downregulates TNFalpha-induced IL-8 production in keratinocytes. *FEBS Lett.* **579**, 3953–3959
31. Kikuchi, G., Yoshida, T., and Noguchi, T. (2005) Heme oxygenase and heme degradation. *Biochem. Biophys. Res. Commun.* **338**, 558–567
32. Powers, J. and Hancock, R. (2003) The relationship between peptide structure and antibacterial activity. *Peptides* **24**, 1681–1691
33. Wakamatsu, K., Takeda, A., Tachi, T., and Matsuzaki, K. (2002) Dimer structure of magainin 2 bound to phospholipid vesicles. *Biopolymers* **64**, 314–327
34. Moore, K., Bevins, C., Brasseur, M., Tomassini, N., Turner, K., Eck, H., and Zasloff, M. (1991) Antimicrobial peptides in the stomach of *Xenopus laevis*. *J. Biol. Chem.* **266**, 1985–19857
35. Reilly, D., Tomassini, N., Bevins, C., and Zasloff, M. (1994) A paneth cell analogue in *Xenopus* small intestine expresses antimicrobial peptide genes: conservation of an intestinal host-defense system. *J. Histochem. Cytochem.* **42**, 697–704